Development of an Experimental Optimization Method in Laser-Assisted Cold Spray

A Major Qualifying Project

submitted to the faculty of

WORCESTER POLYTECHNIC INSTITUTE

in partial fulfillment of the requirements for the

Degree of Bachelor of Science in

Mechanical Engineering

by

Sean Hathaway

_____

Mikhail Khibkin

_____

Matthew Nicholson

_____

March 19, 2017

Approved:

_____

Dr. Diran Apelian, Advisor
Mechanical Engineering

The mission of this project is to develop a new approach to experimental optimization by using theoretical equations to reduce the time it takes to find optimized parameters in a novel materials process currently in research and development.

Abstract

Current experimental optimization methods take extended periods of time and do not have a systematic way to get closer to the optimum. As a result, the team set out to generate a new, systematic approach to experimental optimization that costs time and cost. First, a theoretical goodness equation was used to predict the influential trends of parameters in the Laser-Assisted Cold Spray (LACS) process on three material properties. This was also used to select the algorithm used, Mine Blast Algorithm. The equation and algorithm was then modified for the experimental process which included a fourth variable. The team was able to achieve a goodness of 0.66 after only 5 iterations of the estimated 25 iterations necessary to achieve optimization (30 samples).

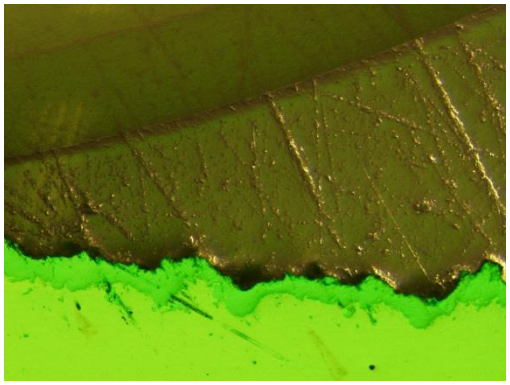

Figure 1. Sample from Iteration 1: Goodness = 0.052, Thickness = 82.35 µm

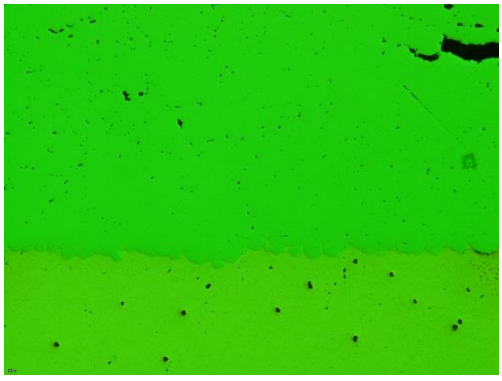

Figure 2. Sample from Iteration 5: Goodness = 0.663, Thickness = 1028.6 µm

Acknowledgements

The team would like to thank IPG Photonics for supporting this project by spraying the samples. The team would also like to thank Aaron Birt for his unwavering guidance and wealth of wisdom throughout the project. Finally, the team would like to thank Diran Apelian for his role in advising this project.

Table of Contents

List of Figures

List of Tables

List of Equations

1.0 Introduction

The purpose of this MQP was to be able to find a more effective methodology to find parameter optimums for material properties. The increased efficiency of the current methodology would decrease time and money spent during testing for materials processes. More specifically with regards to this process, inconel was sprayed onto copper cylinders for several iterations at IPG Photonics in a complex process called Laser Assisted Cold Spray (LACS). A pseudo-predictive equation was initially created based on theoretical information and background research on LACS. This preliminary equation was then used to create an experimental equation that would be used throughout the course of the project to try and find an optimum sample. Using a selected algorithm, the team attempted to optimize several different parameters in the LACS process. The optimum would be the best combination of these parameters that would produce the desired properties for the inconel-copper coating. While one of the purposes was to physically find an optimum for the coating, the primary purpose was the process used in order to find an optimum in quicker and with less resources.

The significance of this project is that it could completely change the way that research and development is conducted within the manufacturing and material science disciplines, particularly in fields related to materials manufacturing. The approach that was utilized in this MQP was to first create a “goodness” equation based on given variables - in this case adhesion, porosity, and hardness. The equation was formed based on theoretical mathematical equations. Each variable had it’s own equation broken down into the seven process parameters. These equations were manipulated so that certain variables were isolated, and then the equations were combined in order to create a final goodness equation. In essence, with this new optimization system, the presence of a materials science expert is only required to make this “goodness” equation based on the desires for the material properties. Moving forward in the process, the materials expert can utilize his time elsewhere as other engineers or technicians will be able to carry out the rest of the process.

The parameters that were selected for experimental control in the Laser Assisted Cold Spray process for this project were gas temperature, raster speed, laser position, laser temperature, mass flow rate, number of passes, and index. These parameters were

determined based on prior research of past LACS experiments as well as the team's own experimental results and analysis. Once the parameters were found and selected, they were put into mathematical equations that were then simplified into only four variables. These variables were adhesion, hardness, thickness, and porosity. With only four properties being analyzed based on seven parameters, it was possible to find new iterations based on desired characteristics through the use of MATLAB. The process was planned to be repeated for 25 iterations until an optimum was found, thus fulfilling the two main purposes of the project. These purposes being that the optimum process parameters were found, and a new process of optimization was a success.

Another vital part of the process is the use of computer software to be able to quickly find the optimum for the given properties. Using the MATLAB code for the selecter optimization algorithm, Mine Blast Algorithm, the optimum combination of parameters should be able to be found in 150 total samples or less. When compared to the fact that most other material property optimization requires more than 400 samples, it is evident that the new system utilized in this MQP would greatly increase overall efficiency. With less than half the number of samples, companies would save money in a variety of ways.

There would be less money going into machine operation costs, as well as less of a chance of damages due to less time on the machines. Companies could even cut down on the total number of workers they have in this area, or at least have them work on other tasks. This makes the company as a whole more efficient, and would save them money from labor costs.

2.0 Background

In cold spray and laser-assisted cold spray, parameters have varying and non-linear effects on the final product in different ways. By looking at these effects, the team was able to create a pseudo-predictive equation to test many different optimization algorithms researched.

2.1 Cold Spray and Laser Assisted Cold Spray

Cold spray (CS) is a novel coating deposition process where coating particles are accelerated at high velocities towards a substrate. Upon impact, the coating particles undergo significant plastic deformation and adhere to the substrate. The main advantage of CS over other coating processes is that it allows for the coating of thermally sensitive components. Specifically, CS allows for the preservation of the functionally required crystallographic structure of the underlying substrate, while transferring the material properties of the coating to the exterior. The velocity needed to induce sufficient plastic deformation of the particles can be reduced by implementing a laser directed at the point of collision between the particle and substrate. This process is known as Laser Assisted Cold Spray (LACS) and is depicted in Figure 3. Other advantages of Cold Spray are depicted in Figure 4.

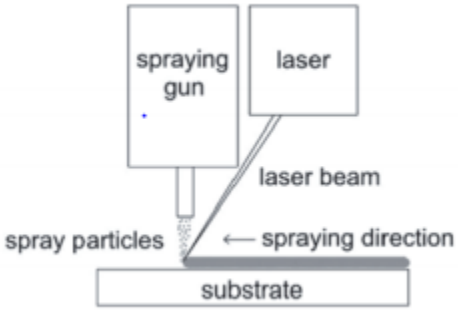

Figure 3. Depiction of Laser-Assisted Cold Spray [1]

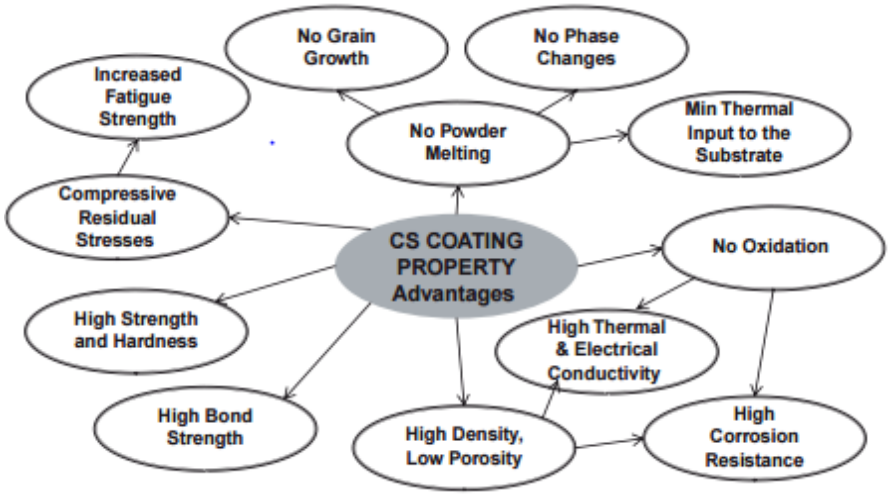

Figure 4. Advantages of Cold Spray [2]

2.1.1 Adhesion Mechanism of LACS

There are two primary methods in which particles can adhere to the substrate. Initial spraying of the substrate results in particles embedding into the substrate, Figure 5. [2] This is one of the mechanisms for adhesion. With continual passes of the spray gun over previously sprayed substrate, the classic adhesion mechanism of CS becomes apparent.This is the second mechanism of adhesion. The particles collide with previously sprayed particles and undergo significant plastic deformation. The interface between the substrate and particle is instantaneously converted into a vacuum and they two-flash weld together. Particles bonding in this manner also experience a high flow stress due to a recursive softening of the particle. Upon impact the plastic deformation releases heat and softens the colliding particle and allows for even further plastic deformation. The resulting coating has an extremely high density of dislocations and thus results in a hard material. This ensures that subsequent deposition of particles onto the incrementally growing coating will adhere in a similar method. This second adhesion mechanic is depicted in Figure 6.

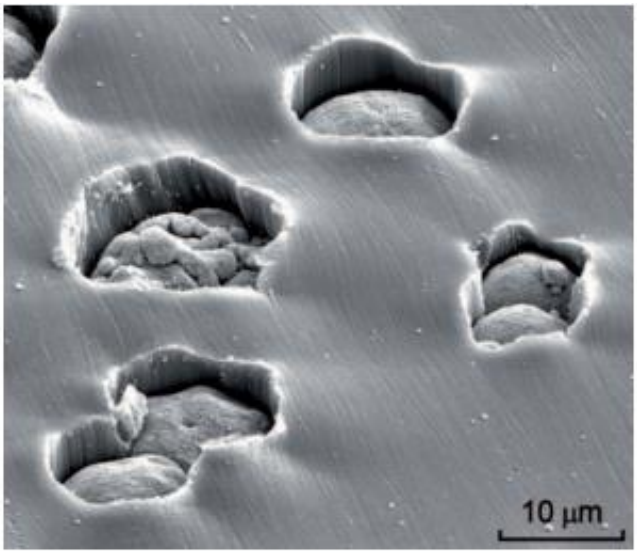

Figure 5. Sprayed Powder Particles Embedded in the Substrate [2]

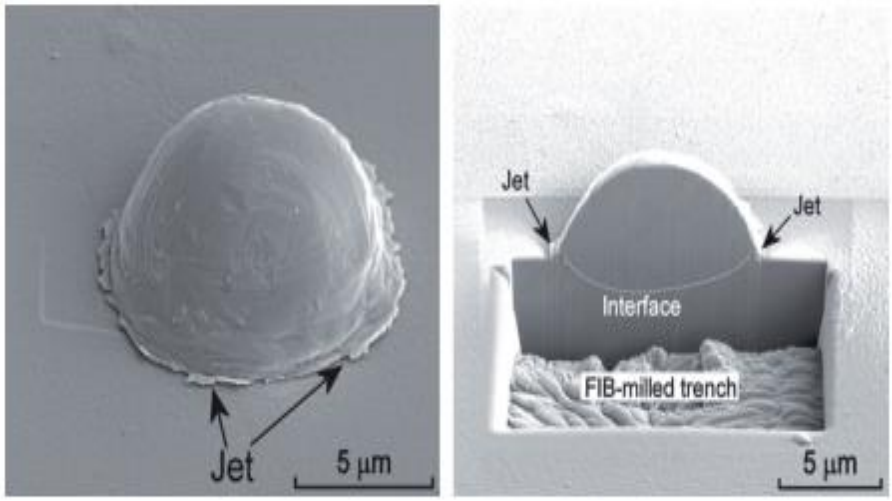

Figure 6. Adhesion Due to Plastic Deformation [2]

2.1.2 Influential Process Parameters in LACS

The following section introduces the parameters of LACS. Subsequently, a table displays the effects these parameters have on the coating.

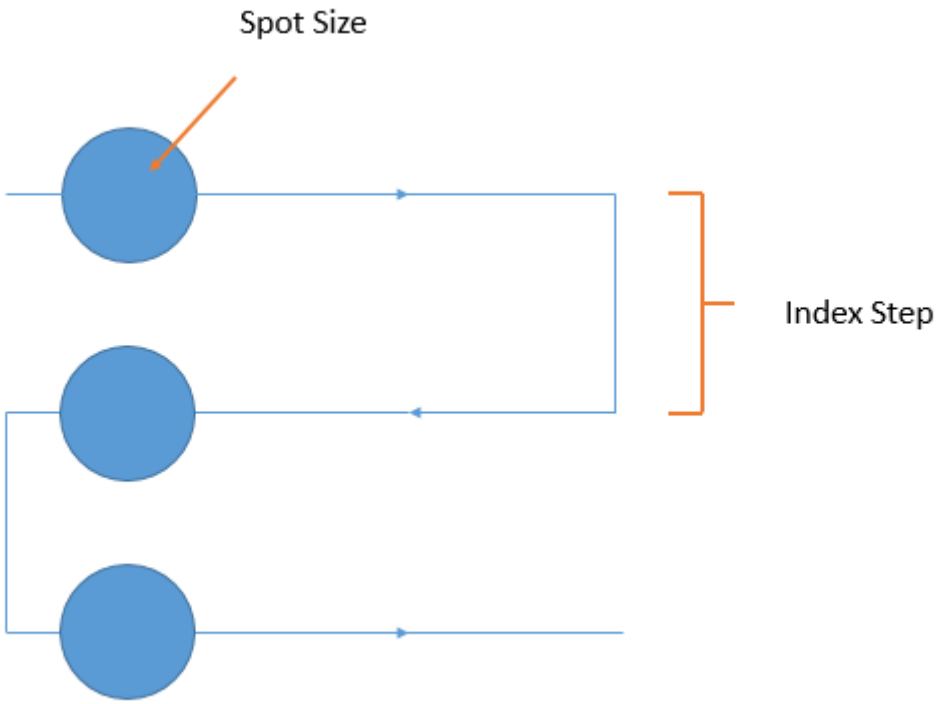

Figure 7. Depiction of Spot Size and Index Step In LACS

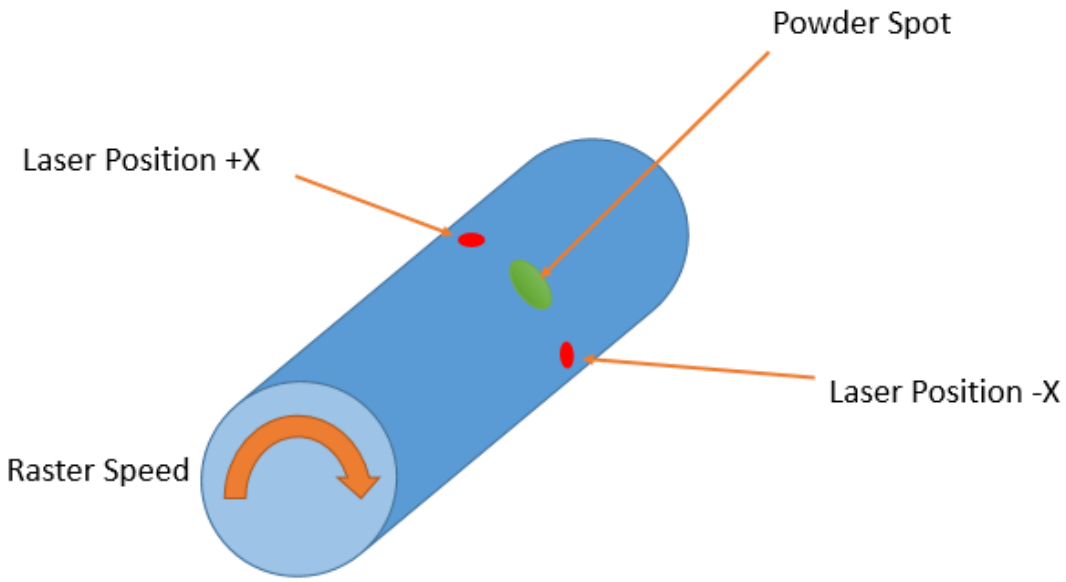

Figure 8. Depiction of Raster Speed and Laser Position in LACS

Raster Speed	The linear velocity at which the substrate work peice moves relative to the spray spot. The biggest effect this has is on the amount of time the laser remains in one spot. Raster speed also affects the powder profile of the coating. In cases where the raster speed is slow the deposition of powder will build up and cause the spraying of the next raster to be deposited on angle. Faster raster speeds mean more evenly deposited powder profiles.
Index Step	Index Step is the amount of space between rasters. The higher the index step the less time there is for the laser to impart heat onto the substrate. A lower index means the laser is spending more time in one spot.
Gas Temperature	Gas Temperature predominantly affects the particle temperature and the particle velocity. Since Cold Spray uses a de Laval nozzle to accelerate the particles, the temperature of the gas is directly proportional to the velocity of the particles. Furthermore, the temperature of the gas also affects the temperature of the substrate due to convectional cooling. As the gas hits the substrate the velocity of the gas affects how much heat it can carry away from the substrate.
Laser Set Temperature	Laser Set Temperature is the amount of heat that is being produced by the laser and directed at the particle/substrate interface. This has a large impact on the critical velocity of the particle.
Laser Position	Laser Position is how far from the cold spray nozzle the laser is aimed at. If the value is positive then the laser is leading the deposition area by the nozzle. If the value is negative then the laser is trailing the deposition area. This has a large effect on a delicate balance between annealing the deposited particles and softening the particles that are impacting the substrate.

Spot Size	Spot Size is the diameter of the laser located on the deposited substrate. This has a large effect on the amount of time the particles have to cool and the powder profile of the particles being deposited on the substrate. This is largely due to the fact that particles that hit the substrate outside of the laser will not deposit. This contributes to low deposition efficiency.
Mass Flow Rate	Mass Flow Rate is the mass flow rate of a metalic powder through the LACS nozzle. It is a parameter that affects all of the previously stated parameters. A few examples of this is that a higher mass flow rate requires a higher gas temperature and laser set temperature to allow for deposition of particles. Additionally, a high mass flow rate and low raster speed creates a wavy coating as the powder will be deposited in shelve like structures. In this way mass flow rate has a large impact on all of the parameters in LACS.

2.2 Optimization Algorithms

Conventionally, optimization algorithms find optimal solutions to a given problem. Each algorithm can generate different results depending on its structure. The most common types of algorithms are gradient-descent and global optimization algorithms. Gradient-descent algorithms are first-order algorithms designed to follow gradients to reach either a maximum or minimum. The function for these must be continuous and differentiable. Since this method follows gradients and only starts at one point, the algorithm typically finds a local minimum or maximum rather than a global minimum or maximum. Examples of these in the team's investigation is "Fmincon" and "Fminimax." Figure 9 also shows an example of a path that a gradient-descent algorithm would follow [4]. The other types of algorithms examined were global optimization algorithms. Examples of these include genetic

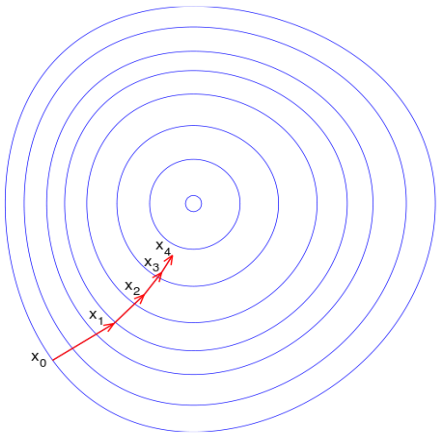

Figure 9. Example of a Path a Gradient-Descent Optimization Algorithm Could Follow [3]

algorithms, simulated annealing, pattern search, particle swarm, and mine-blast algorithm. These algorithms use different methods which are designed to find global maximums and minimums, rather than a local maximum or minimum. Most of these algorithms are more versatile as they do not require the function to be continuous or differentiable, however they are not guaranteed to find the global maximum or minimum. Finally, these can be either population based or non-population based in a single iteration. Figure 10 shows an example of a global optimization algorithm.

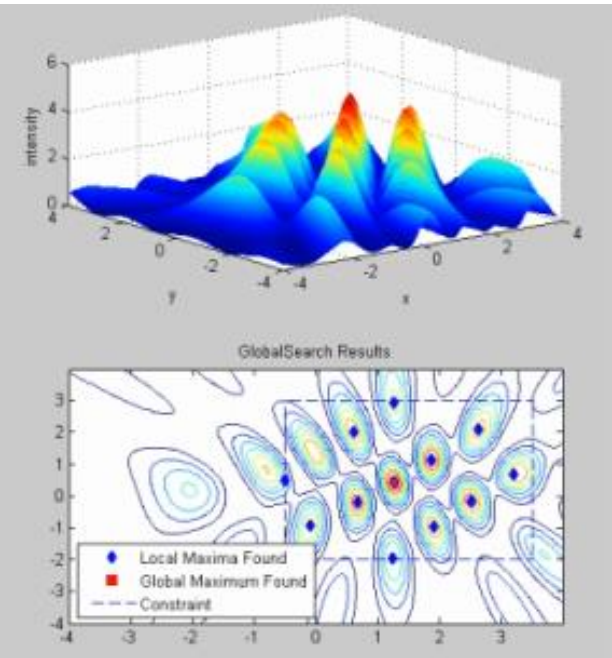

Figure 10. Example of a Global Search Algorithm to Finding a Global Optimum Over a Local Optimum [5]

2.2.1 Fmincon and Fminimax

Fmincon and Fminimax are nonlinear, gradient-descent problem solvers which are designed to find a minimum of a differentiable and continuous function [6,7]. Each iteration has only one function evaluation in it. The algorithms start at a user specified point and the next iteration is randomly generated with a specified step size. The algorithm produces an iteration which moves in the direction towards a minimum. If the function evaluation is not getting smaller, the iteration will randomly generate a new sample until it does. The algorithms will continue this process until the evaluated function has exhausted the directions it can travel as the difference between the last moved point and the current point is less than a defined tolerance. The only difference between the two algorithms is Fminimax can solve problems that are not smooth while Fmincon requires a smooth function [6,7].

While this algorithm is fairly straight forward, it has many limitations to it. The biggest limitation is the types of functions it requires. The objective function must be both continuous and differentiable. As equations become more complex, and not continuous or differentiable, there is a much higher chance of the algorithm not producing the correct

results or a local minimum when a global minimum is required. Another limitation is its time to convergence. As it gets closer to the minimum, it may take many iterations to get the right direction to advance. Finally, the algorithm may not be ideal as only one function evaluation (sample) may be made at a time before advancing.

2.2.2 Simulated Annealing

Simulated annealing is algorithm that mimics the process of annealing in which a material is heated up to reform its crystal structure by removing dislocations and slowly cooled to produce a refined microstructure. This global optimization algorithm generates a new point in each iteration starting from a single, user-input point. It uses a probability distribution that is proportional to a temperature scale, like in annealing [5]. With the goal of minimizing the function, points that lower the function value are accepted and are used in the next iteration. The algorithm will also accept points, with a low probability, that are worse to expand the search space. The algorithm continues this process and reanneals (raises the temperature back up to begin the lowering process again) until the function evaluation no longer improves [8,9].

Since this algorithm uses probability, it is still possible that it will not reach a global maximum depending on the starting point, but it is much more likely to reach the global optimum [9]. This process is also timely as the function may be evaluated several times before it can move to the next iteration if the acceptance criteria are not met.

2.2.3 Pattern Search

Pattern search optimization is a global optimization algorithm that does not require the function to have a gradient, be continuous, or be differentiable [10]. It uses meshes to find an optimum. A mesh consists of points which expand from a starting point of the iteration. The algorithm starts at one specified point and a mesh is generated. This mesh starts large and gets smaller with time. Each mesh contains points that explore the solution space at a specified distance in each direction. When one of the mesh points are less than the starting point of the iteration, the algorithm adopts it as the next starting point. If none of the points improve from the starting point, the mesh size is reduced and

a new set of points is generated [10]. This process continues until an optimum is found.

One of the limitations of this algorithm is possibly finding a local optimum. It is possible that the meshes do not expand enough out and miss the area of the solution space that contains the global optimum. Another limitation is if the solution space is large, it may take an enormous amount of time to reach the optimum as it will need to cover a large area [10].

2.2.4 Genetic Algorithm

Genetic algorithm is one of the most popular global optimization algorithms. This algorithm begins with a randomly generated population. Each point in the population is evaluated and a fitness value is given to it. A few points from each population get selected and are identified as “parents” for the next iteration based on their desired fitness values. New points are generated based on the “parent” points through random changes (mutation) or combining parents (crossover). This process continues until the optimum is found [8].

One of the limitations to this algorithm is the population size. A large population is able to cover a large section of the solution space, but it may take longer to converge to the optimum. Another limitation is that there is no guarantee to find a global optimum. The initial population may not be near the global optimum, so it will converge to a local optimum if it does not expand from the initial area [11].

2.2.5 Particle Swarm

Particle swarm optimization is a population-based optimization algorithm which mimics the behavior of animals that travel in swarms or flocks (eg. birds) [8]. The algorithm starts by randomly generating a population of points that cover a large portion of the search space and gives each point a position and velocity. In each iteration, these points are evaluated and the best function value (the lowest value when trying to minimize) and the best neighbors are determined. Based on each point’s position and velocity, a new population is generated which moves towards each of these best points [8]. As the iterations advance, the velocities become smaller and the population begins to converge

towards the optimum.

As a population based algorithm, its time to convergence and ability to find the global optimum is dependent on the population size. A large population will cover the solution space more completely and will be able to find the global optimum better and faster. As the population size is reduced, it has a chance of not covering the entire search space and miss an area that has the global optimum and converge to a local optimum [12]. As a global optimization algorithm, the algorithm is able to solve functions which are discontinuous and nondifferentiable.

2.2.6 Mine Blast Algorithm

Mine blast algorithm is a new population based global optimization algorithm. It is designed to mimic explosions of land mines with shrapnel being the different points being evaluated [13]. This algorithm has two phases to it: exploration and exploitation. The algorithm starts with the “first shot” which can be randomly generated or user selected. From here, the exploration phase begins with randomly generated points based around the “first shot.” Each point from the “first shot” are at random distances from it, but are equally spaced in outward directions. The exploration phase has much larger distances to explore the solution space and it does not directly focus on the best point. However, after the exploration phase, the points begin to converge towards the optimum in the exploitation phase. The distance of the points begin to decrease until it reaches essentially zero [13]. When this distance reaches zero, it has converged to the optimum.

This algorithm, just like the other population based algorithms, is dependent on the population size. When the population size is larger, the solution space is more thoroughly explored and there is a greater possibility of finding the global optimum. However, it is not guaranteed to find the global optimum if it does not explore enough, or the population size is too small [13]. Another limitation is that it is so new. Due to its young age, all of its possibilities and limitations have not been explored. However, the basis of this algorithm allows for a wide range of functions to be used.

3.0 Approach

The overall approach this project was run can be broken down into six different steps, as seen in Figure 11. First, an overarching theoretical goodness equation was created based on background research. Next, optimization algorithms were tested and one was selected that would be able to locate a maximum for the observed parameters in a short number of samples and iterations. Once these two were selected based on analyses, they were adjusted so that they could be used for the purpose of the experiment. Next, samples were characterized and measured to calculate the goodness. The fifth step was to input the calculated goodness values into the MATLAB program, and then have the program generate new samples. These fourth and fifth steps were repeated for 5 iterations. Finally, the results were recorded and analyzed.

Figure 11. Flow Chart of the Project Approach

3.1 Development of Pseudo-Predictive Equation/Parameter Influences

The theoretical equation uses both experimentally and theoretically driven relationships between seven parameters of cold spray to predict a goodness value of an LACS coating. This goodness value lies between zero and one, and is a consolidation of 3 different factors which were deemed to be the most influential through the help of Aaron Birt, an expert in the technology of LACS. The three influential factors are influence of adhesion ($I_{adhesion}$), influence of porosity ($I_{porosity}$), and influence of hardness ($I_{hardness}$). This section subsequently lays out the relationships which comprise each of these influences and addresses the methods in which they were developed. The overall equation is presented first for reference and reiterated after each section for clarity.

Equation 1. Overall Goodness Equation

$$Goodness =$$

$$= \begin{cases} 1, & 667 - .014\rho + .08(T_m - T_R) + 10^{-7}\sigma_u - 0.4(T_i - T_R) \geq .8 * \sqrt{\frac{TR}{M}\frac{2\gamma}{\gamma - 1}\left[1 - \left(\frac{P_e}{P}\right)^{\frac{\gamma-1}{\gamma}}\right]} \\ 0, & 667 - .014\rho + .08(T_m - T_R) + 10^{-7}\sigma_u - 0.4(T_i - T_R) < .8 * \sqrt{\frac{TR}{M}\frac{2\gamma}{\gamma - 1}\left[1 - \left(\frac{P_e}{P}\right)^{\frac{\gamma-1}{\gamma}}\right]} \end{cases}$$

$$* \left\{ 1 - \frac{\sqrt{\frac{TR}{M}\frac{2\gamma}{\gamma - 1}\left[1 - \left(\frac{P_e}{P}\right)^{\frac{\gamma-1}{\gamma}}\right]} - 2(V_{crit})}{2(V_{crit})} \right\} * \{1 - \frac{H_{expected} - H_T}{H_T}\}$$

3.1.1 Influence of Adhesion on Goodness Equation

The goodness of a coating is dependent on the ability of the cold spray particles to properly remain adhered to the surface of the substrate. The adhesion of particles was reflected in the equation by attributing a binary value to ($I_{adhesion}$). This value was equal to one for coatings which remained adhered to drive the goodness value to unity. Conversely, the value was zero to ensure that coatings which did not adhere to the substrate were unable to contribute anything but zero during the calculation of the goodness value.

The binary value was predicted by comparing the expected velocities of the cold spray particles to the critical velocity found in literature which facilitated coatings. Tobias Schmidt et al [14] developed the following equation to determine the aforementioned critical velocity with the respective parameters found in the table immediately after.

Equation 2. Critical Velocity in Cold Spray Particles

$$V_{crit} = 667 - .014\rho + .08(T_m - T_R) + 10^{-7}\sigma_u - 0.4(T_i - T_R)$$

Where:

ρ = Density of Material

T_m = Melting Temperature of Material

T_R = Reference Temperature (During Project the temperature used was room

temperature)

σ_u = Yield Stress of Material

T_i = Impact Temperature of Particle

The material properties for both inconel 625 and copper were input into Schmidt's equation [14] to predict the critical velocity necessary for a coating to adhere. The rationale behind predicting the critical velocities for both materials is that there were two foreseeable scenarios in which the particles would adhere to the copper. In the first scenario inconel particles would embed themselves into the copper substrate. The copper substrate would deform plastically and allow the inconel particles to imbed themselves. In this case the material properties of copper were used in the critical velocity calculation. Since the equation for critical velocity is based on particles traveling and deforming there is some error in assuming that the effects would be the same when the copper is in bulk material form. In bulk material form it is more difficult to deform the copper. Thes effects were considered negligable.

In the second scenario, the more conventional plastic deformation of the accelerated LACS particle would cause for the coating adherence. As such, the critical velocity prediction was performed using inconel 625 as a material property.

To predict the velocity the LACS nozzle would propel the inconel particles, the equation for a de Laval nozzle was used. It is derived from the Bernoulli formula. An example of the nozzle is depicted in Figure 12. [15]

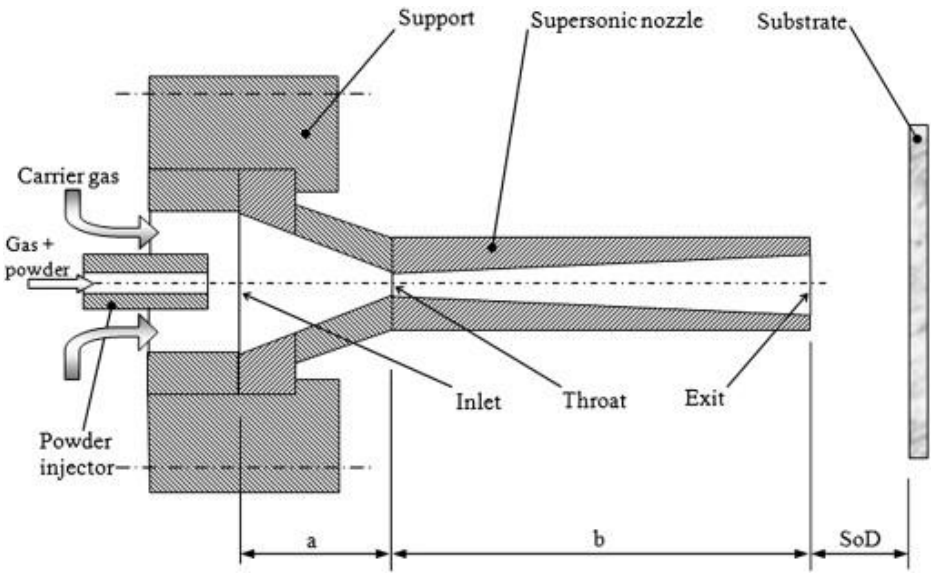

Figure 12. Cold Spray Nozzle [15]

This equation and its associated parameters are listed below.

Equation 3. Velocity of Particles Upon Impact

$$V_{particle\ impact} = .8 * \sqrt{\frac{TR}{M}\frac{2\gamma}{\gamma - 1}[1 - (\frac{P_e}{P})^{\frac{\gamma-1}{\gamma}}}$$

Where:

T = Absolute Temperature of Inlet Gas

R = Universal Gas Law Constant

M = Molecular Weight of Gas

γ = Isentropic Expansion Factor for Gas

P_e = Absolute Pressure of Exit Gas

P = Absolute Pressure of Inlet Gas

The properties of nitrogen gas were used during the calculation of the velocity of the particles. For simplification, the particles were assumed to move at 80% the velocity of the nitrogen gas.

The final step in predicting the binary output for ($I_{adhesion}$) is comparing the critical velocity of both copper and inconel to the predicted ballistic velocity of the inconel particles. A step function would produce a value of one for ($I_{adhesion}$) if the expected velocity of the inconel particles was greater or equal to the critical velocity of copper, the critical velocity of inconel 625, or the average of the critical velocities for copper and inconel 625. Similarly, the complementary half of the step function would produce a zero in all other cases.

Equation 4. Goodness Equation with Impact of Adhesion

$$Goodness1 =$$

$$= \begin{cases} 1, & 667 - .014\rho + .08(T_m - T_R) + 10^{-7}\sigma_u - 0.4(T_i - T_R) \geq .8 * \sqrt{\frac{TR}{M}\frac{2\gamma}{\gamma - 1}\left[1 - \left(\frac{P_e}{P}\right)^{\frac{\gamma-1}{\gamma}}\right]} \\ 0, & 667 - .014\rho + .08(T_m - T_R) + 10^{-7}\sigma_u - 0.4(T_i - T_R) < .8 * \sqrt{\frac{TR}{M}\frac{2\gamma}{\gamma - 1}\left[1 - \left(\frac{P_e}{P}\right)^{\frac{\gamma-1}{\gamma}}\right]} \end{cases}$$

3.1.2 Influence of Porosity on Goodness Equation

The goodness of a coating is also highly dependent on its porosity. Coatings with high porosity are brittle and are not useful in a multitude of applications. To calculate ($I_{porosity}$) research from Schmidt et al. [14] showed that deposition efficiency was maximum at twice the critical velocity. The graph below displays a parabolic curve at which the vertex coincides with twice the critical velocity.

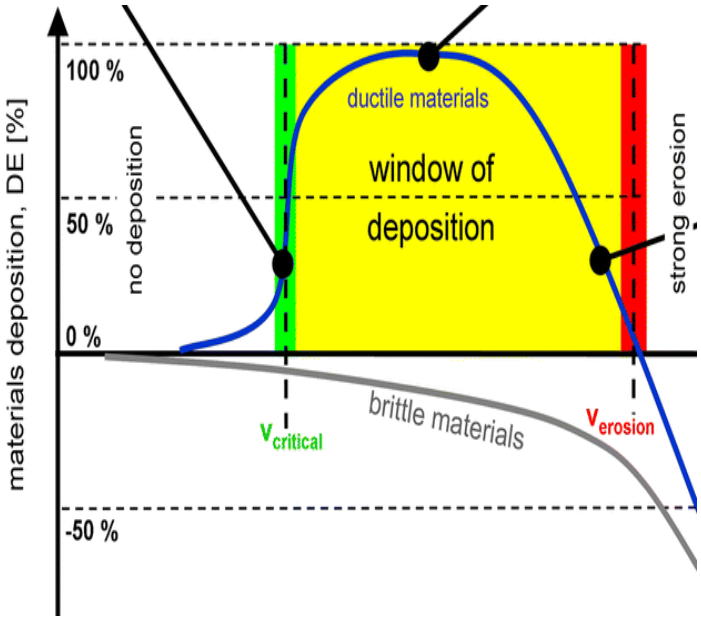

Figure 13. Deposition Efficiency Relating to Porosity [14]

The team chose to assume that deposition efficiency could be used to predict porosity, because any particle that was accelerated to the substrate would either have to bond and form a coating or would fly off and be wasted (Figure 13). When the deposition efficiency was maximum this meant the highest amount of material was colliding with the either the substrate or already adhered inconel particles. In these cases, the particles would experience maximum plastic deformation and subsequently experience the greatest amount of flow stress. As such, this high deposition efficiency and its associated high flow stress would result in a very a low porosity. Thus, the value for ($I_{porosity}$) could be represented in a mathematical relation showing relative distance from twice the critical velocity of inconel particles. This formula is seen below and uses the same equations to calculate the velocity and critical velocity of the inconel particles.

Equation 5. Equation for Impact of Porosity

$$I_{porosity} = \left\{ 1 - \frac{.8 * \sqrt{\frac{TR}{M}\frac{2\gamma}{\gamma-1}\left[1-\left(\frac{P_e}{P}\right)^{\frac{\gamma-1}{\gamma}}\right]} - 2\left(667 - .014\rho + .08(T_m - T_R) + 10^{-7}\sigma_u - 0.4(T_i - T_R)\right)}{2\left(667 - .014\rho + .08(T_m - T_R) + 10^{-7}\sigma_u - 0.4(T_i - T_R)\right)} \right\}$$

Equation 6. Goodness Equation due to Impact of Adhesion and Impact of Porosity

$$Goodness2 = Goodness1 * \left\{1 - \frac{.8 * \sqrt{\frac{TR}{M}\frac{2\gamma}{\gamma-1}\left[1-\left(\frac{P_e}{P}\right)^{\frac{\gamma-1}{\gamma}}\right]} - 2\left(667 - .014\rho + .08(T_m - T_R) + 10^{-7}\sigma_u - 0.4(T_i - T_R)\right)}{2\left(667 - .014\rho + .08(T_m - T_R) + 10^{-7}\sigma_u - 0.4(T_i - T_R)\right)}\right\}$$

3.1.3 Influence of Hardness on Goodness Equation

3.1.3.1 Choosing a target Hardness

Optimal hardness in material coatings is a frequently desired material property. Basic material science dictates that a metal will become more brittle as the hardness increases due to the higher density of dislocations. Since the principle behind this project was to show the optimization strength of computer algorithms as opposed to optimizing for a specific application the group selected an optimal hardness based on intrinsic material properties of inconel 625. The optimal hardness in this project was selected using the hardness value associated with the highest toughness value for inconel 625. This value was derived by integrating the area under a stress-strain curve for the material as seen in the diagram, Figure 14.

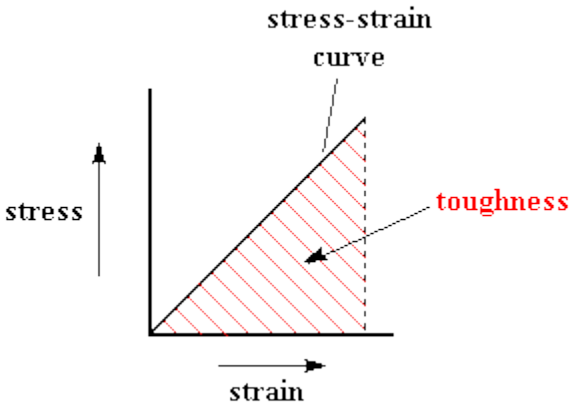

Figure 14. Method of Finding Toughness

The toughness for inconel was estimated by finding toughness values for both the data gathered from materials testing of the yield strength and ultimate tensile strength of inconel. This data is presented in Table 1. 209 was chosen as the optimal hardness.

Table 1. Cold Work Relating to Hardness [15]

Cold Reduction, %	Tensile Strength		Yield Strength (0.2% offset)[b]		Elongation %	Reduction Of Area, %	Hardness	
	ksi	MPa	ksi	MPa			Rockwell C	Vickers
0	115.5	796.3	49.5	341.3	67.0	60.4	88 Rb	179
5	121.0	834.3	77.5	534.3	58.0	58.1	94 Rb	209
10	130.0	896.3	102.5	706.7	47.5	54.6	25	257
15	137.0	944.6	112.5	775.7	39.0	51.9	32	309
20	143.0	986.0	125.0	861.8	31.5	50.0	34	326
30	165.0	1137.6	152.0	1048.0	17.0	49.3	36	344
40	179.5	1237.6	167.0	1151.4	12.5	41.9	39	372
50	189.5	1306.6	177.0	1220.4	8.5	38.0	40	382
60	205.0	1413.4	180.5	1244.5	6.5	32.7	44	427
70	219.0	1510.0	201.0	1385.8	5.0	25.4	45	440

To estimate the toughness of inconel from these two tests the graph of the stress-strain curve was assumed to take the form presented in figure. The values for the .2% strain offset and cold reduction percent were used as the values for yield stress and tensile stress respectivley, Figure 15.

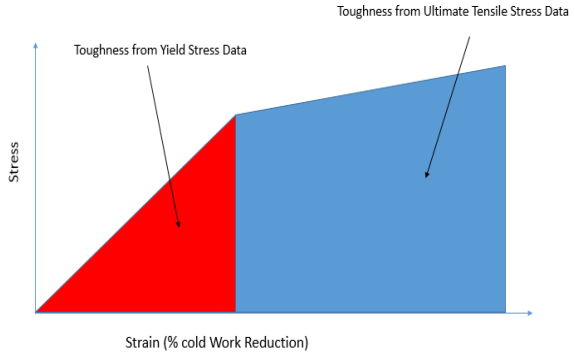

Figure 15. Toughness

The area under these graphs was then calculated using symple geometric formulas for a triangle and trapezoid. After calculating the toughness of inconel the hardness was correlated to the tests, by again, using Figure 16. Toughness was then plotted against hardness and it was found that the maximum toughness coressponded to a value of 15 on the Rockwell B hardness scale. This is the value that was used for the desired hardness.

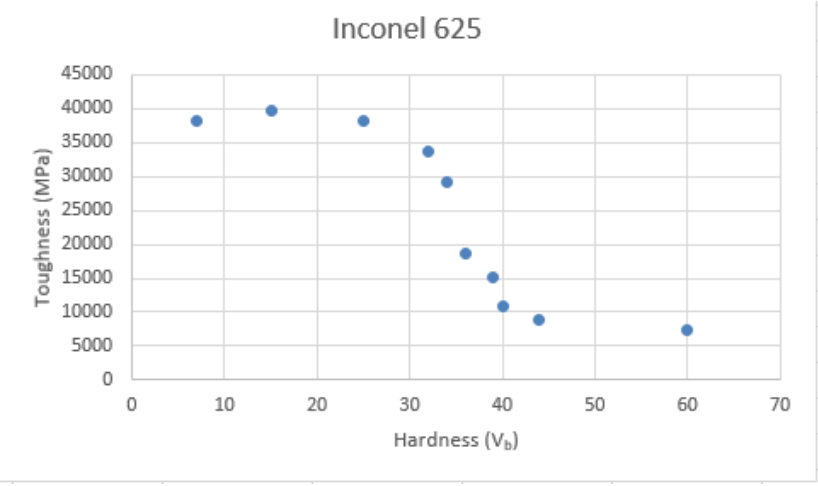

Figure 16. Hardness vs. Toughness

Analogous to section 3.1.2, the value for ($I_{hardness}$), in the overall goodness equation, was calculated by

creating a relationship describing the relative difference between the desired hardness and expected hardness. This relationship is given below with H_T being the optimal target hardness of 15.

Equation 7. Simplified Impact of Hardness

$$I_{hardness} = 1 - \frac{H_{expected} - H_T}{H_T}$$

3.1.3.2 Predicted Expected Hardness Using Experimental Data

Due to the novelty of LACS it was difficult to predict the expected hardness theoretically as a function of parameters. The prediction was instead formulated empirically through the analysis of a set of samples created using an orthogonal variation of LACS parameters in an attempt to determine the effect each individual parameter had on the hardness. After initial screening for potential relationships between hardness and each individual parameter clear relationships could not be determined. The team reanalyzed the samples and attempted to find correlations between cold work percent and parameters based on the intuition that a relationship between cold work percent and hardness could be developed based on classic material science principles. In order to measure the cold work percent of the samples an optical micrsocope at 100x magnification was used to randomly select discernable particles from a coating. Two diameters of this particle were selected, as shown in Figure 17, and the area of the elipse was calulcated using the formula $A = \pi * D_1 D_2$. This area was compared to the known average area of the particles prior to depostion. The relative change between these two values was found and used as the percent cold work using the equation:

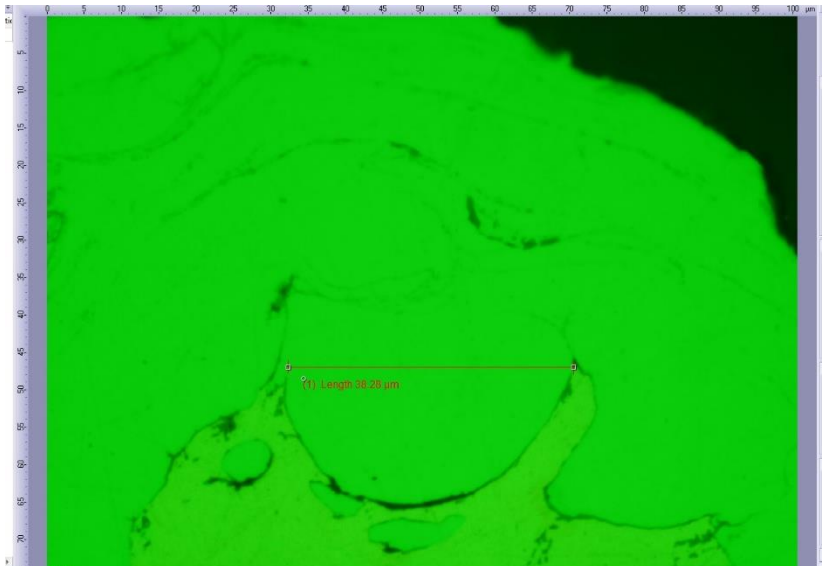

Figure 17. Measured Diameter of Cold Spray Particle

Equation 8. Calculation of Percent Cold Work

$$\%\ Cold\ Work = \frac{Original\ Area - Area\ of\ deposited\ Particle}{Original\ Area}$$

Cold work was then plotted against hardness to identify relationships between the two values. As seen in Figure 18, there were two identifiable trends that the samples followed. The difference between these two trends was the rate of variation of hardness with percent cold work (slope of the projected lines).

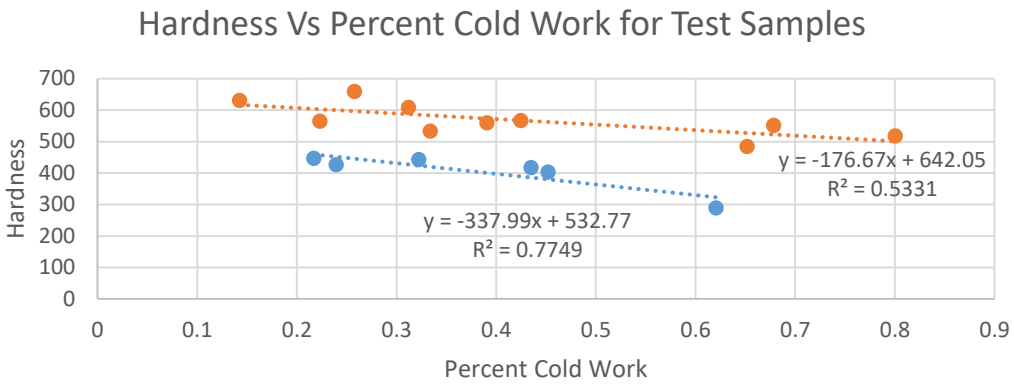

Figure 18. Identifiable Trends in Cold Spray Parameters

The samples were thus split into two groups. Group A being the blue line and Group B being the orange line. Laser Position was investigated as the primary reason for the two trends in the lines. The immediate correlation was found for both lines with laser position as seen in Figure 19. Samples from both group A and B with a trailing Laser had a trend line that was lower in cold work than samples with a leading laser. No other correlations could be found between other parameters and cold work in samples with a trailing laser.

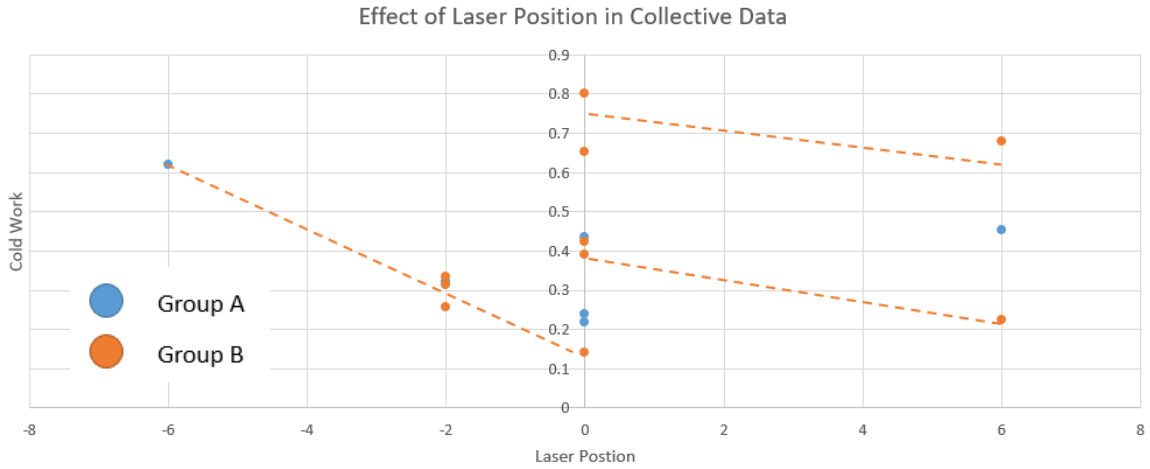

Figure 19. Differences Between Trailing and Leading Laser

The relationship is most likely a result of the laser energy annealing the coating when trailing the spray and softening the particles when leading the spray allowing for more plastic deformation and consequently percent cold work. This was integrated into the predictive equation by using a piecewise function to create two different predictive equation for if the laser was trailing or leading. This essentially allowed for predicting the reason that two trend lines were seen in the percent cold work versus hardness graph. The individual effects of the parameters in a leading laser were further analyzed by plotting the value for the parameters with a leading laser against cold work and giving these graphs trendlines (Figure 20). There were two trend lines in these samples. One trendline had a lower percent cold work than the other and is designated Line 1. These samples are the same as those seen in Figure 19 on the lower right side. The line directly above it is Line 2.

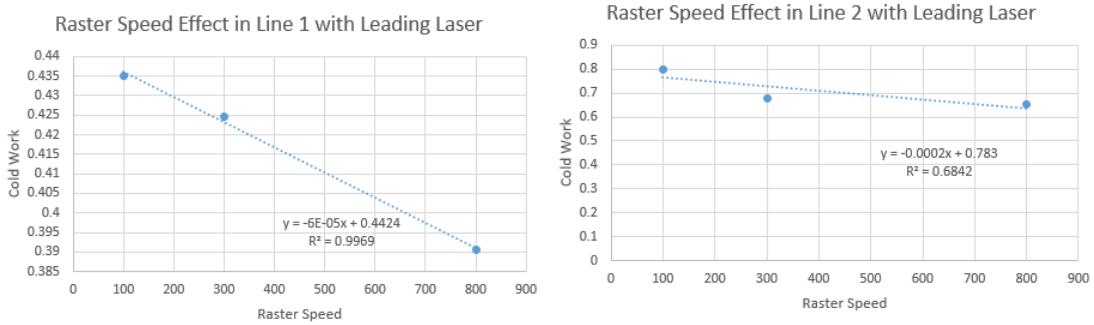

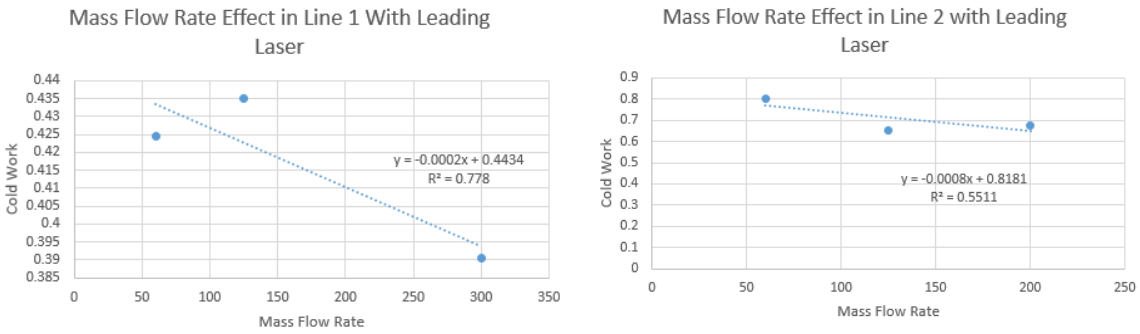

Figure 20. Trends Between Mass Flow, Raster Speed, and Percent Cold Work

The final step was to multiply all of these equations together to get the experimentally predicted effect of parameters on percent cold work in group B. The last step was to find the relationship between percent cold work and hardness to tie the parameters in with hardness. This can be seen in Figure 21.

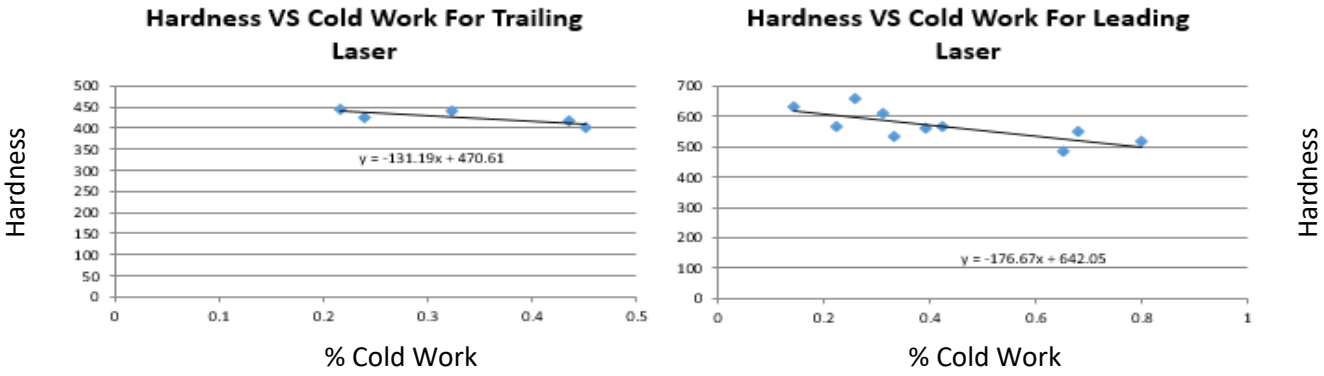

Figure 21. Equations Relating Hardness and Percent Cold Work For Trailing and Leading Laser

By relating the effects of the cold spray parameters to the expected hardness the impact of hardness was able to be calculated. The equation is lengthy to be fit and has been attatched in Appendix A for reference. The final equation shown below is only representative of the principle that the goodness of a coating is calculated. The addition of the hardness component to the equation is meant to show the indicative relationship that the computer algorithm uses; not the exact calculations the algorithm performs.

Equation 9. Simplified Overall Goodness Equation

$$Goodness = Goodness1 * Goodness2 * \{1 - \frac{H_{expected} - H_T}{H_T}\}$$

3.2 Optimization Algorithm Evaluation and Selection

After creating the pseudo-predictive equation, the testing of different optimization algorithms began. The equation was made into a MATLAB function script to be easily applied to the seven different algorithms. To determine which algorithm would be the best, three different measures were examined. The first was the algorithm's ability to find the global optimum rather than a local optimum. Each algorithm went through five trials of different starting points. If the algorithm's optimum goodness value significantly changed over these trials, that was an indication of the algorithm's inability to find the global optimum. Figure 22 shows the trials of each algorithm. Since Fmincon, Fminimax, Genetic Algorithm, and Simulated Annealing had changing goodness values, these algorithms were ruled out of the selection process as they will not always converge to a global optimum.

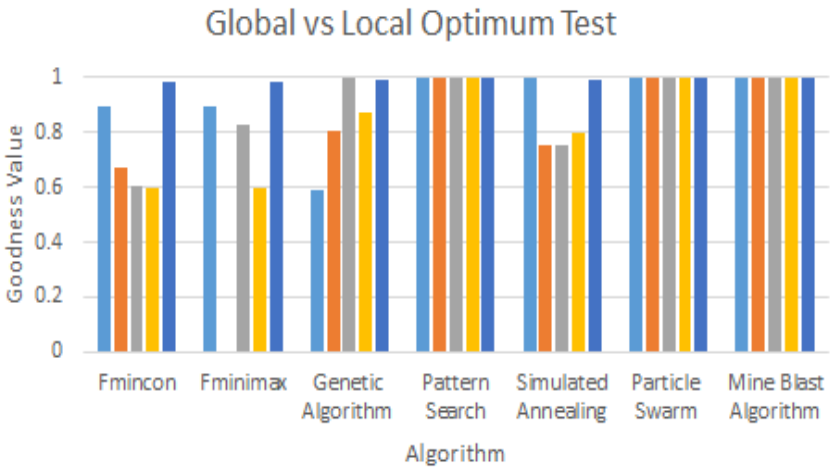

Figure 22. Results of Five Trials to Determine if Algorithms Converge to a Global or Local Optimum

The next measure was the number of function evaluations it took for the algorithm to converge. Since current experimental optimization practices take approximately 400 samples to find the optimum, an algorithm required under 400 function evaluations to be considered. This rules out pattern search and simulated annealing from the final selection, as seen in Figure 23. Going hand-in-hand with function evaluations is iteration size. Since some algorithms are not

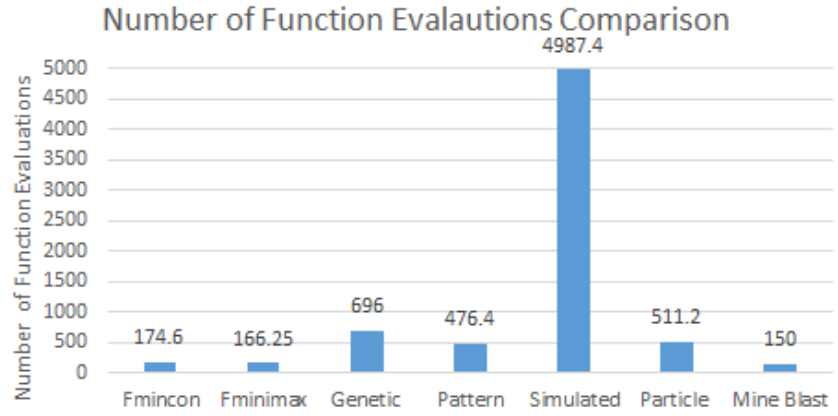

Figure 23. Comparing the Average Number of Function Evaluations to Find the Optimum for Each Algorithm

population based, it would require significant time to prepare one sample, characterize it, and then generate the next sample. Due to the timeliness of that process, algorithms should have larger population sizes.

After each of these were examined (Table 2), the final optimization algorithm selected for this process was the Mine Blast Algorithm (MBA). This algorithm seems to typically converge to a global optimum and it required only 25 six-sample iterations totaling 150 samples. This algorithm will spend four iterations in the exploration phase, as aforementioned, and the remainder will exploit the optimum.

Table 2. Comparing the Seven Algorithms Goodness, Iteration Size, and Function Evaluations

	Fmincon	Fminimax	Genetic Algorithm	Pattern Search	Simulated Annealing	Particle Swarm	Mine Blast Algorithm
Average Goodness	0.751557	0.82588	0.8517634	0.999805	0.8606074	0.999933	1
Iteration Size	1	1	6	1	1	6	6
Average Function Evaluations	174.6	166.25	696	476.4	4987.4	511.2	150

3.3 Equation and Algorithm Adjustments

The main focus of the pseudo-predictive equation was to determine which algorithm would optimize the parameters of LACS most efficienctly to create a coating with the desired material properties. To extend the functionality of this optimization process the equation was adjusted to also drive the coatings towards the desired dimensional and economical properties. This was reflected in the algorithm through the use of expected and desired thickness values.

$$Goodness = I_{adhesion} * I_{porosity} * I_{hardness} * I_{expected\ thickness} * I_{desired\ thickness}$$

For each iteration the thickness of the coating was characterized through optimcal imaging and compared to the predicted thickness of the coating and the desired thickness of the coating. By comparing the predicted thickness of the coating to the actual thickness the deposition efficiency of the parameters were determined. Similar to $I_{porosity}$ and $I_{hardness}$ the impact of deposition efficiency was characterized through the equation:

$$I_{Depostion\ Efficiency} = \frac{|Expected\ Thickness - Actual\ Thickness|}{Actual\ Thickness}$$

The expected thickness was predicted through the use of the following equation. Essentially this equation determines the volume of material deposited on the sample and then devides by the surface area of the sample to produce and expected thickness.

$$Expected\ \text{Thickness} = \frac{\dot{m} * \text{Spot Size}^2}{\text{SA} * \rho^* \text{Raster} * \text{Index}}$$

Where:

$\dot{m}$ = Mass Flow Rate

Spot Size = Size of Nozzle Spray

SA = Surface Area of the Sample Being Sprayed

ρ = Density of Powder Material

Raster = Raster Speed

Index = Index Step Size of Sample

Through the use of these two equations a value between .9 and 1 was assigned to $I_{expected\ thicknes}$ and subsequently used to drive the parameters towards coatings that yielded less wasted product and were economically preferable. The purpose behind setting a lower cap of .9 was to ensure that at least some influence made the coatings more economic with each iteration, however, did not interfere with a coating that was exceptional in other regards.

A similar value was also assigned to $I_{desired\ thickness}$. This value, however, was between 0 and 1 similar to the other impact equations. It was used to drive the coatings towards the disired value of 1mm thick in order to demonstrate that the process could simultaneoulsy allow for geometric restriction of the coating when optimizing for the other material and economic properties with the computer algorithm.

After adjusting the equation, the MBA also had to be adjusted to allow for user input and the new equation. The need for goodness calculations in the algorithm were replaced with the ability to input the goodness value for a certain sample. Figure 24 shows what this process looks like to the user. After the user enters all the goodness values for

the completed iterations, the algorithm generates the next iteration of sample parameters. These parameters then move into production and characterization.

```
Parameters of Iteration 1
      650          1000             6          1400      288.77211      12.591231      3.3900295
 556.3639      118.98967     2.0634897          1400      170.75673             15      4.0974198
538.21065      86.364905            -6           400              1              1            0.1
404.23859             20            -6           400              1      5.5610912            0.1
      250      58.067404            -6     1197.8214      44.552403      7.2732663            0.1
      650      218.02884             6     1374.4612      135.43141       10.54819      1.7181274
Your current sample number in this iteration is 1
What is the goodness value of the above sample?
```

Figure 24. MATLAB Displaying the First Iteration Parameters and Requesting the First Sample's Measured Goodness Value

3.4 Sample Production and Characterization

The fourth step of the overall process for this MQP was the characterization of the samples. This was the step that required physical lab work to be completed by the group so that the adhesion, porosity, hardness, and coating thickness could be found. Aaron Birt would spray inconel onto a copper cylinder based on the parameters given for a certain iteration at IPG Photonics. Each iteration would have six different samples that underwent Laser-Assisted Cold Spray with varying parameters. These parameters would be selected based on the MATLAB optimization algorithm that took the previous iteration's goodness results into account. After spraying the samples, they would be brought to WPI for characterization.

Once the iteration was obtained, the procedures for actually characterizing the different samples would begin. First, the cylinder would be cut into six small segments by using a circular abrasive saw to cut out a thin sliver. Once this thin piece was cut out of the cylinder, it was then cut horizontally into six pieces that would then be utilized for characterization. These six pieces would be set in an epoxy solution that would harden and hold the samples in place so that they would be easier to handle moving forward with the characterization process.

The six samples would remain in the epoxy for several hours until the solution was completely solid. From there, the samples would be polished to remove any possible scratches. There were four different pads used in the polishing process, each one getting progressively thinner than the one used before it. After this process was finished, the

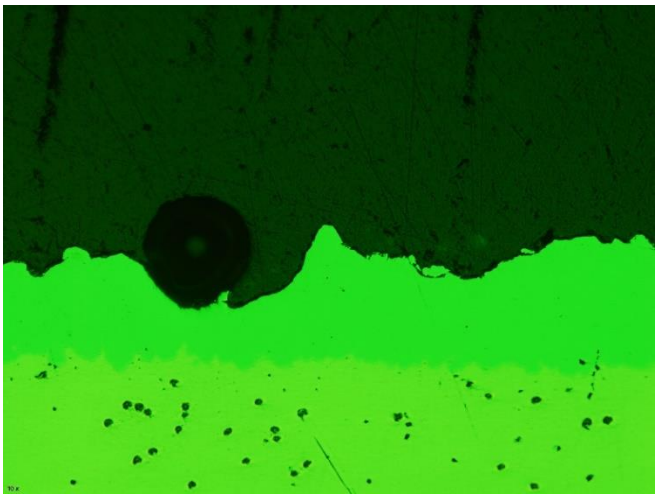

Figure 25. Image of Adhered Coating Under Microscope

samples were observed under a microscope to ensure that the scratches had been removed. After the samples were deemed satisfactorily polished, they could then be taken to be imaged. The samples were taken under a microscope, and snapshots were taken of the inconel coating. The snapshots were taken horizontally from left to right so that there would be overlap between each image. If the coating was so wide so that the entirety of it could not be captured from one horizontal strip, then the images would start from the bottom of the coating left to right, then move up at the end of the row, and come back right to left on the new, higher row. These snapshots were uploaded to a computer so that they could be analyzed.

From these images, the thickness could be measured from the computer program that the images were taken on. Five random points on the coating were measured, and then averaged for an overall thickness. For adhesion, the images were looked at to see if there truly was a coating along the edge of the sample, Figure 25. If not, then the adhesion was given a 0. If so, the adhesion was given a 1. Next the images were stitched together using a macro. The macro would stitch them together, then straighten out the images so that a long line that roughly reflected the entire length of the sample was created. Using this fused image, the porosity macro was run and gave a result between 1 and 0, with 0 representing no holes in the coating, and 1 meaning only holes in the coating. After all these were completed, the samples could then be tested for hardness by using a Vickers Hardness test which indents the coating as seen in Figure 26. In the same manner that coating

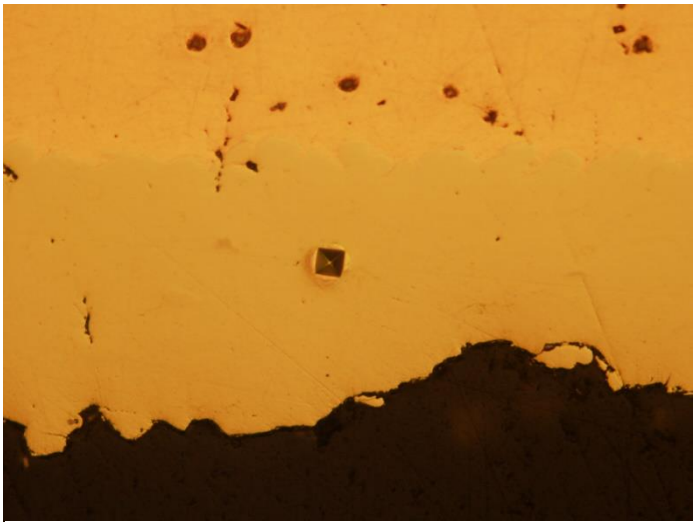

Figure 26. Image of Indentation from Vickers Test

thickness was found, the hardness was found by performing the Vickers test on five random locations in the coating, and the average of those five results was used as the overall hardness. Once these four properties were measured, the Goodness could be calculated for each of the six samples.

After carrying out several iterations, a random group of five samples that had already been tested were reevaluated in the same procedure. This was done to try and prove that the properties found for each sample were inherently true for that specific sample, and not just a coincidence based on the polishing and imaging done initially. From the beginning of the project, it had been assumed that each of the properties obtained from the tested samples was truly representative of the sample, and the sensitivity testing was done to verify or refute this assumption.

To test for this, one random sample was taken from each of the first five iterations. Two trials were conducted: one by polishing the original mounted sample again, and another by cutting and mounting the sample again. After this, the aforementioned procedures were conducted to find the new hardness, porosity, thickness, adhesion, and goodness values.

3.5 Report Findings

The final step of the process was to simply communicate the findings for each iteration with IPG Photonics so that another algorithmically dictated iteration of six samples could be produced. Steps 4-6 were repeated several times as the Mine Blast Algorithm predicted 150 total samples (25 iterations), to find an optimum. Based on the results found from each iteration, general feedback on certain aspects of the samples were provided. For example, if any one or more of the samples were impossible to spray due to the shear amount of time or spray that would have to be used, he would make that clear to the group. Communication between the advisor and group members was essential during the course of this project, and was necessary to be able to get iterations done as efficiently as possible.

4.0 Results

The immediate visible trend in the data is that the average goodness value of each iteration increases. This can be seen in Figure 27 and Figure 28.

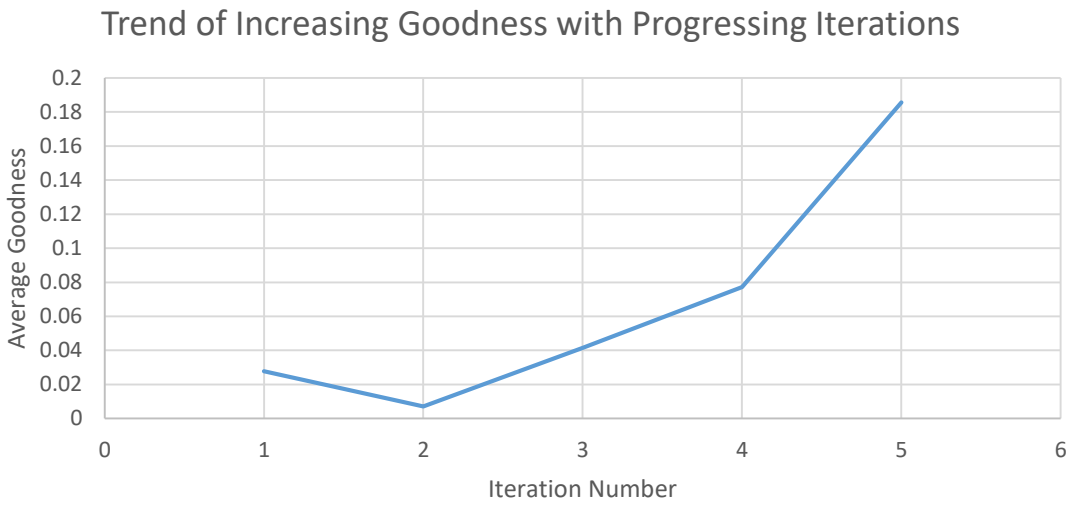

Figure 27. Goodness as a Function of Iteration

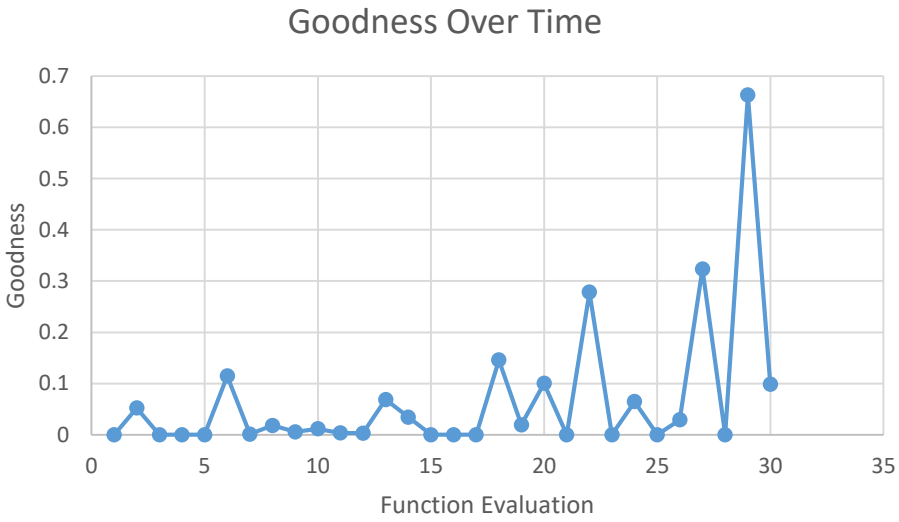

Figure 28. Goodness of All Function Evaluations or Samples

The parameters of the best sample in each iteration has been taken and graphed in a radial plot to visualize the way in which the algorithm changes the parameters. Besides each of these radial plots the goodness for the associated sample has been graphed out of a total of 1. Both these graphs were created by normalizing the values of

the parameters to be on a scale of 100 with the lower and upper constraints for the parameters equivalent to 0 and 100 respectively. Goodness was already normalized to have a scale of 0 to 1. This scale is still used with a 1 being the maximum target goodness.

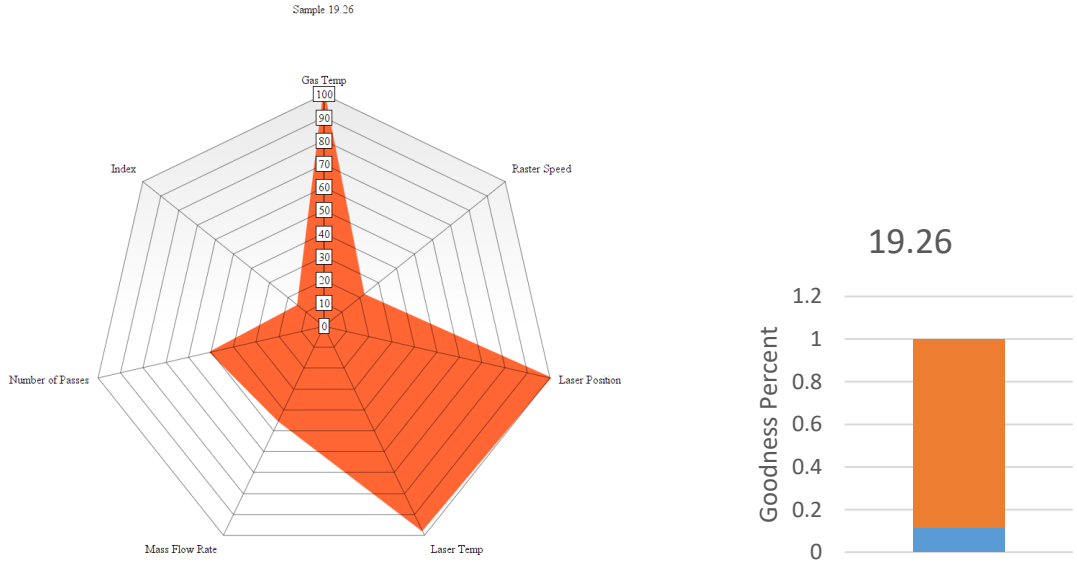

Figure 29. Visualization of Sample 19.26 Parameter Values and Goodness

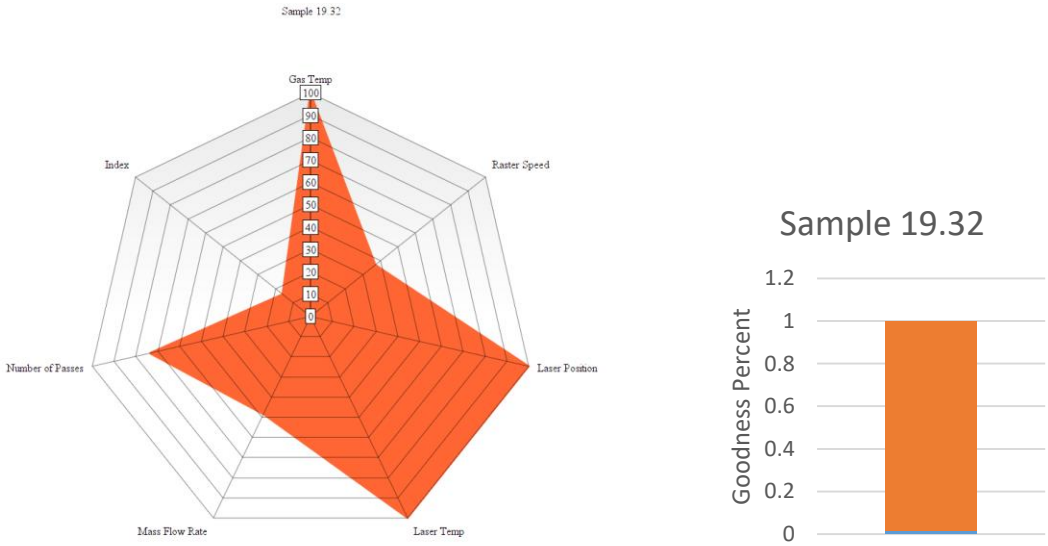

Figure 30. Visualization of Sample 19.32 Parameter Values and Goodness

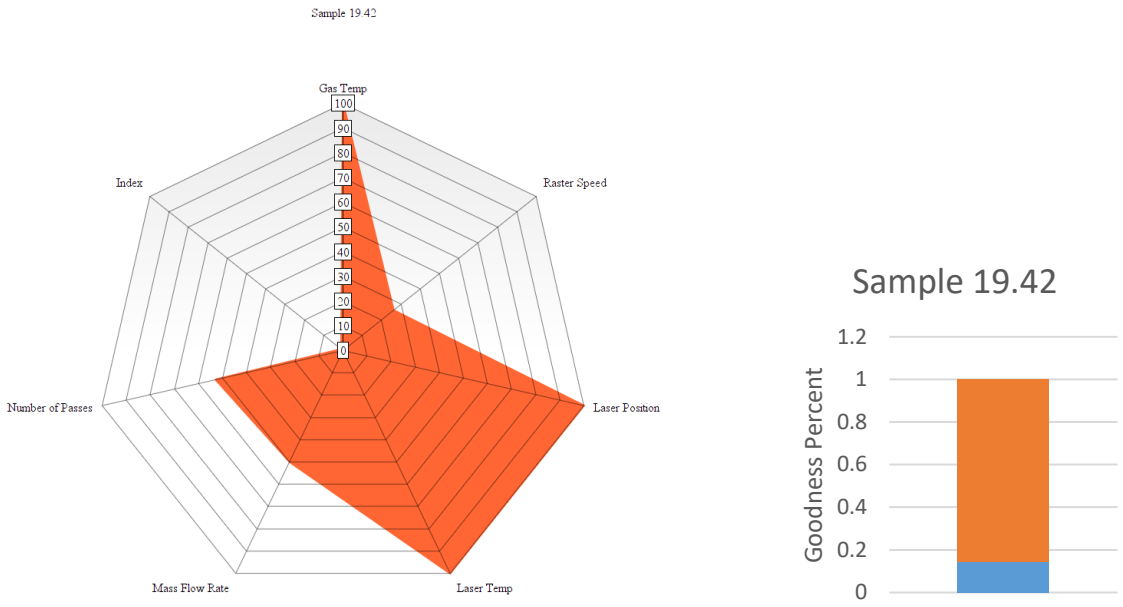

Figure 31. Visualization of Sample 19.42 Parameter Values and Goodness

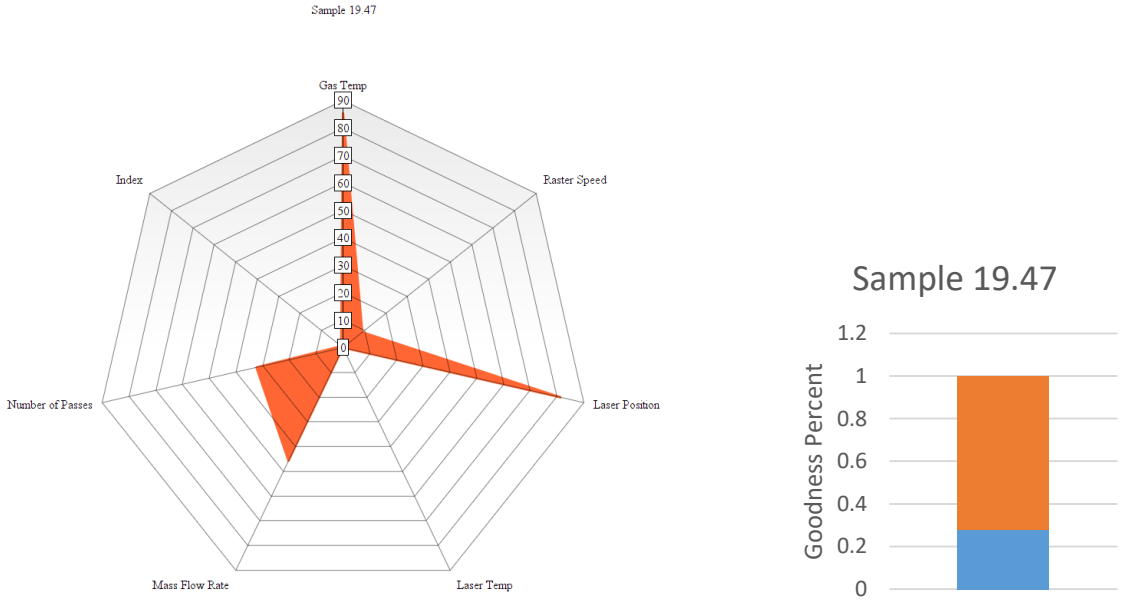

Figure 32. Visualization of Sample 19.47 Parameter Values and Goodness

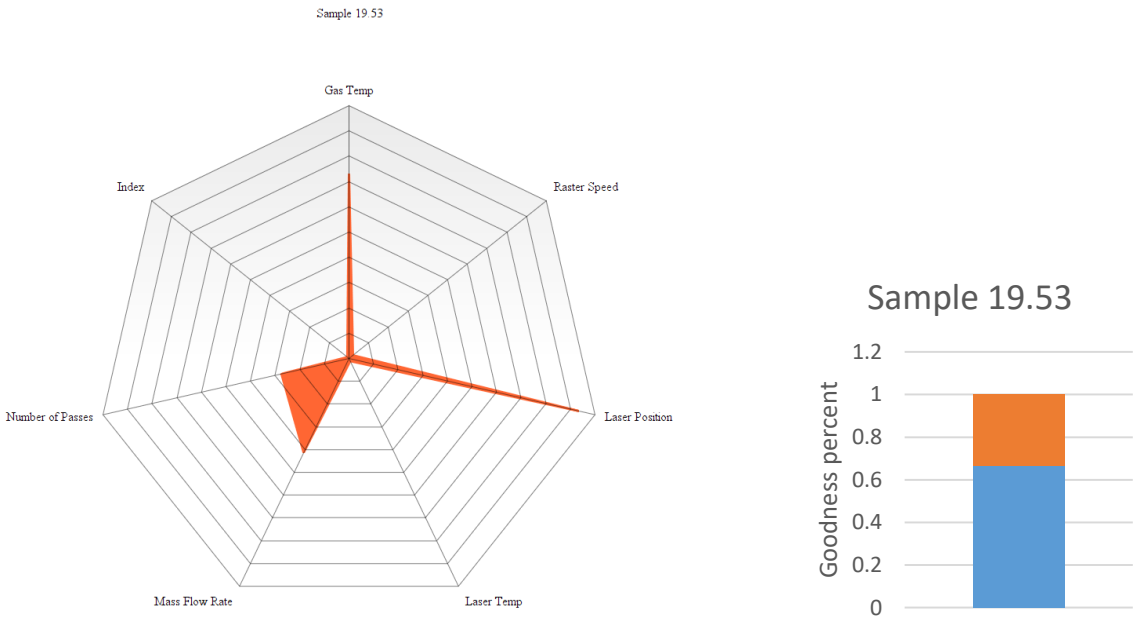

Figure 33. Visualization of Sample 19.53 Parameter Values and Goodnes

4.1 Sensitivity Analysis

It was important to verify whether or not the measurements taken were representative of the enter coating. When the five samples were repolished, there was an average difference between the original and new sample of 0.055. However, one sample was an extreme outlier in which its goodness value more doubled, so when ignoring the outliar, the average is only 0.0115. This indicates that while there is a difference after grinding off a thin layer it is not very significant. To look more in depth as to why it may have changed, we look at the other variables of the goodness equation.

Since only a thin layer was grinded off, the thickness of the samples did not change. However, when looking at hardness, there was an average difference of 130.66 Vickers. This was much more significant of a change. However, the thickness of a couple coatings were very thin, under 100 µm, so the hardness test may have bled into the epoxy or substrate and may not be representative of the whole sample. Additionally, porosity may have had a significant effect on hardness. For example, Sample 19.47 had an original porosity of 0.135 and a hardness of 601.2 Vickers. After being repolished, the porosity dropped to 0.013 and the hardness became 417 Vickers. A significant decrease in hardness was experienced potentially due

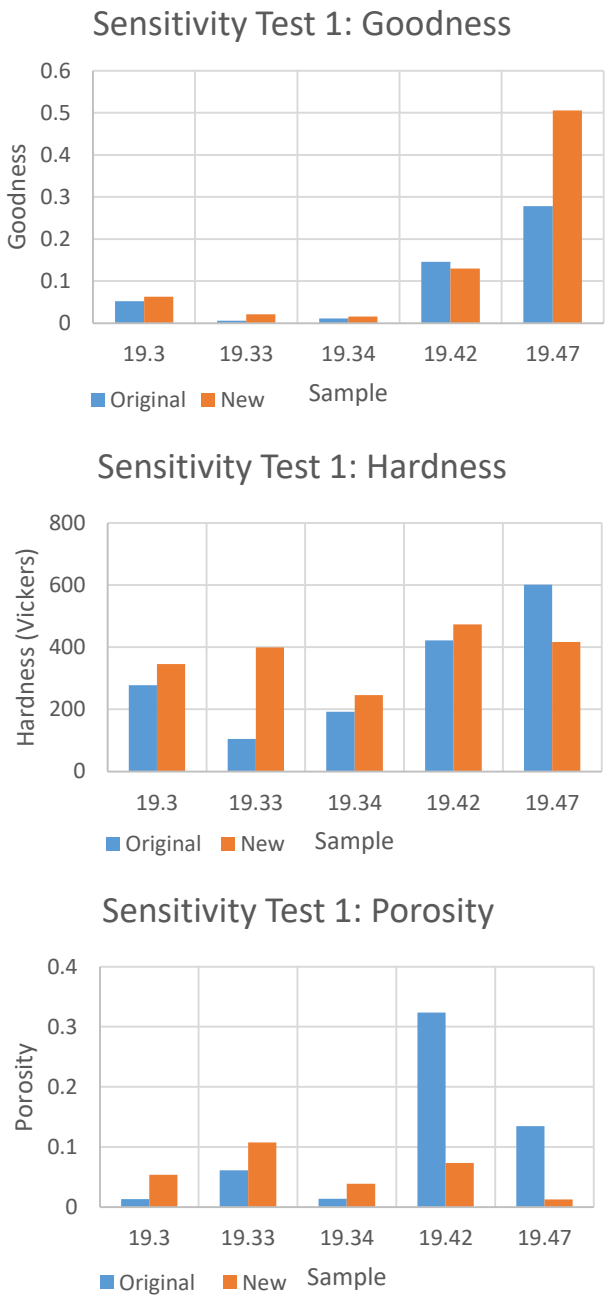

Figure 34. Sensitivity Test by Reploishing Results

to the coating being less porous. Finally, porosity had an average change of 0.097. This is less significant of a change, but this could be due to user error. The team experienced difficulties with polishing for the first couple iterations. After experience, the polishing improved and may have improved the porosity images which would decrease the porosity reading. The individual results of the sensitivity test can be seen in Figure 34.

Furthermore, the team tested the sensitivity by cutting a new sample and taking measurements. Two of the samples were retested after the first sensitivity test, and two are new samples. In terms of goodness, there was not a significant change. The average change in goodness was 0.015 which is fairly insignificant. However, the change was larger when comparing hardness. The average change in hardness was 66.21 Vickers. However, Sample 19.33 had a significant change in hardness, likely due to its thin coating, which is not seen as much in the other samples. Next, the changes in porosity were fairly significant. Three of the four samples had a significant difference in the porosity readings. These could be due to imaging or polishing errors. Finally, the thicknesses changed unlike when the samples were just repolished. The average change in thickness was 26.54 µm. Figure 35 shows the details of the second sensitivity test.

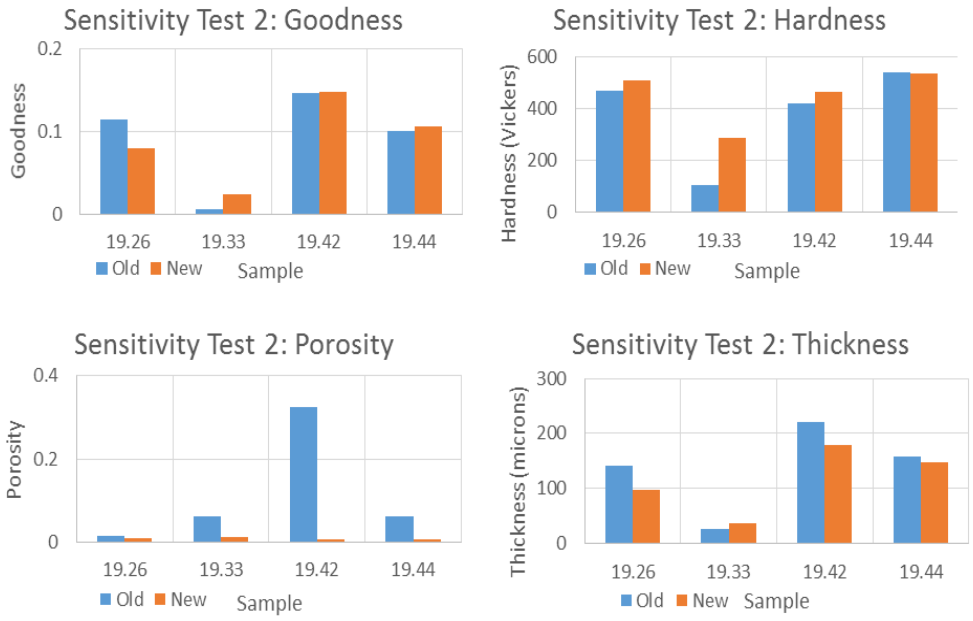

Figure 35. Sensitivity Test by Recutting Results

All in all, the samples seem to have relatively close goodness values, which is the target, as seen in Figure 36. The few exceptions could be due to a number of errors in the experimental process, such as a user learning curve in polishing and imaging, or

limitations in the size of the coatings. In conclusion, the samples seem to not vary enough which indicates the measurements are not very sensitive to measurement location.

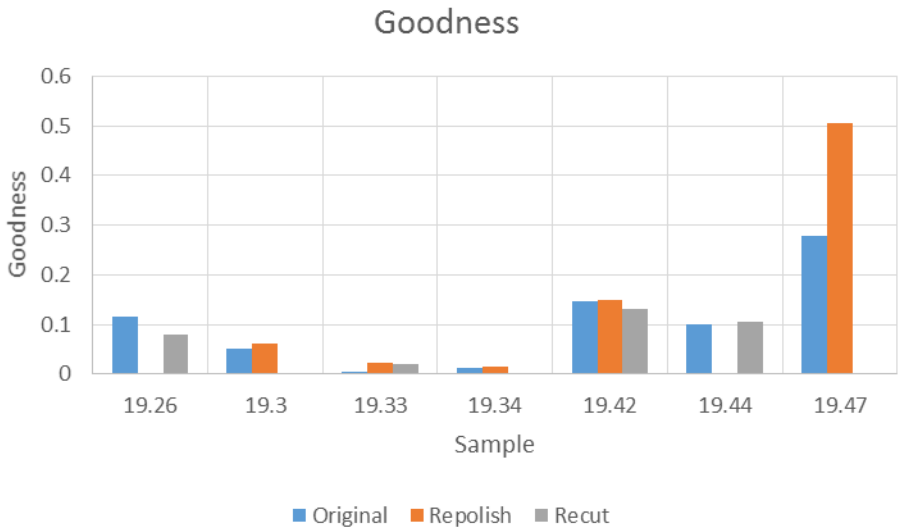

Figure 36. Comparing Goodness for All Samples

5.0 Conclusion and Future Work

The experiment conducted in this MQP was done primarily to attempt to create a new process in which to optimize material samples that undergo Laser Assisted Cold Spray. To try and accomplish this end state, a pseudo-predictive equation was prepared, followed by an experimental equation that was created based on theoretical knowledge and research. These equations found a goodness value for the individual samples, and an optimization algorithm was selected to try and get each iteration to have a higher goodness than the iteration preceding it.

The goal at the beginning of this project was to have a total of 25 iterations with 6 samples in each iteration. Due to constraints, only 6 iterations were able to be completed. Despite not reaching our initial goal as far as number of samples, we saw that the goodness value of each progressive iteration got higher. As a whole, the Inconel-copper coatings continued to adhere, became thicker, less porous, and had surfaces with a hardness near the desired hardness, which were the four variables of interest in the project. The graphs of goodness versus iteration showed a positive correlation, which we had hypothesized would be the case. It was concluded that this process can be utilized to improve iterations over time, but due to the number of iterations completed the optimum sample was not attained. After creating the first four iterations, the group wanted validation that the properties collected for each sample were truly representative and not just by chance based on the preparation procedures. So, two variation iterations were completed; one iteration was re-polishing 4 previously made samples, and the other was completely recutting 4 samples from previously made coatings from IPG Photonics. The conclusions for both of these iterations were the same, that the properties collected were representative. When the Goodness values were compared with the values from the initial samples' experimenting, it was evident that the values were comparable enough to validate that there was not variation. Aside from a couple of the samples having a much lower porosity than what was originally found, the other properties were very similar.

For future work, this group would like to see more iterations be carried out so that a more accurate pattern of the iterations' improvement can be analyzed. The groundwork has already been done, but at this point more samples would have to be created and then characterized to see if the optimum was reached in the initially hypothesized 150 samples

(25 iterations). Another future work possibility would be to try this process out again but with different parameters in the goodness equations, or a different coating combination than Inconel-copper. Since a brand new optimization process is trying to be created, it is important to get a wide sampling of different combinations to prove or disprove that the process truly finds an optimum efficiently.

References

[1] Christoulis, D. and C. Sarafoglou. "Laser-Assisted Cold Spray". *Modern Cold Spray* (2015): 275-302. Web.

[2] Villafuerte, J., SpringerLink (Online service), & SpringerLINK ebooks - Chemistry and Materials Science. (2015). Modern cold spray: Materials, process, and applications (1st 2015.;1st 2015; ed.). Cham: Springer International Publishing. doi:10.1007/978-3-319-16772-5

[3] https://en.wikipedia.org/wiki/Gradient_descent

[4] Kiwiel, Krzysztof C. "Convergence And Efficiency Of Subgradient Methods For Quasiconvex Minimization". *Mathematical Programming* 90.1 (2001): 1-25. Web.

[5] "Global Optimization Toolbox". *Mathworks*. N.p., 2017. Web.

[6] "Fmincon". *Mathworks*. N.p., 2017. Web.

[7] "Fminimax". *Mathworks*. N.p., 2017. Web.

[8] Weise, Thomas. Global Optimization Algorithms - Theory And Applications. 2nd ed. 2009. Print.

[9] Ingber, L. "Adaptive Simulated Annealing (ASA): Lessons Learned". *Control and Cybernetics* (1995): n. pag. Print.

[10] Kolda, Tamara G, Robert Michael Lewis, and Virginia Torczon. "Optimization By Direct Search: New Perspectives On Some Classical And Modern Methods". *SIAM Review* 45.3 (2003): 385-482. Web.

[11] "Genetic Algorithm". *Mathworks*. N.p., 2017. Web.

[12] "Particle Swarm". *Mathworks*. N.p., 2017. Web.

[13] Sadollah, Ali et al. "Mine Blast Algorithm: A New Population Based Algorithm For Solving Constrained Engineering Optimization Problems". *Applied Soft Computing* 13.5 (2013): 2592-2612. Web.

[14] Schmidt, T., Gärtner, F., Assadi, H., & Kreye, H. (2006). Development of a generalized parameter window for cold spray deposition. Acta Materialia, 54(3), 729-742. doi: 10.1016/j.actamat.2005.10.005

[15] R. Lupoi and W. O'Neill. Powder stream characteristics in cold spray nozzles. *Surface and Coatings Technology 206(6),* pp. 1069. 2011. doi: 10.1016/j.surfcoat.2011.07.061.

[16] Inconel Alloy 625. 2013. Web. http://www.specialmetals.com/assets/documents/alloys/inconel/inconel-alloy-625.pdf

Appendix A - Full Theoretical Goodness Equation

Goodness=

$$\begin{cases} 1, & 667 - .014\rho + .08(T_m - T_R) + 10^{-7}\sigma_u - 0.4(T_i - T_R) \geq .8 * \sqrt{\frac{TR}{M}\frac{2\gamma}{\gamma - 1}\left[1 - \left(\frac{P_e}{P}\right)^{\frac{\gamma-1}{\gamma}}\right]} \\ 0, & 667 - .014\rho + .08(T_m - T_R) + 10^{-7}\sigma_u - 0.4(T_i - T_R) < .8 * \sqrt{\frac{TR}{M}\frac{2\gamma}{\gamma - 1}\left[1 - \left(\frac{P_e}{P}\right)^{\frac{\gamma-1}{\gamma}}\right]} \end{cases} \begin{cases} 1 \\ -\frac{.8 * \sqrt{\frac{TR}{M}\frac{2\gamma}{\gamma - 1}\left[1 - \left(\frac{P_e}{P}\right)^{\frac{\gamma-1}{\gamma}}\right]} - 2(667 - .014\rho + .08(T_m - T_R) + 10^{-7}\sigma_u - 0.4(T_i - T_R))}{2(667 - .014\rho + .08(T_m - T_R) + 10^{-7}\sigma_u - 0.4(T_i - T_R))} \end{cases}$$

$$* \begin{cases} 294 - (642.05 - 176.67 * (1 - 2.484 * 10^5) \\ * \frac{\frac{(Gas\ temp * number\ of\ passes)^2}{Gas\ temp^2 * Raster\ Speed * Index} * e^{\frac{-98}{8.314 * Gas\ temp * laser\ temp}}}{3.13159 * 30^2} * (.7056 \\ + \frac{(-.0012 * Gas\ temp * \dot{m} - 5.7142 * 10^{-4} * \text{Gas temp} * \text{Raster Speed}}{2}, \quad laser\ position \geq 0 \end{cases}$$

$$294 - (532.77 - 337.99 * (1 - 2.484 * 10^5) * \frac{\frac{(Gas\ temp * number\ of\ passes)^2}{Gas\ temp^2 * Raster\ Speed * Index} * e^{\frac{-98}{8.314 * Gas\ temp * laser\ temp}}}{3.13159 * 30^2} * (.55 + \frac{(.002 * Gas\ temp * \dot{m} - 2.791 * 10^{-4} * \text{Gas temp} * \text{Raster Speed}}{2}, \text{ laser position } < 0$$